Research Article Vol. 4, No. 9 / 15 Sep 2021 / OSA Continuum 2481

Enhanced narrowband mid-IR thermal radiation enabled by plasmonic stacked gratings

YUSUF ABUBAKAR,[1] YONGKANG GONG,[2,*] DUN QIAO,[1] YUANLONG FAN,[1] CHRISTOPHER EVERED,[1] ADAM JONES,[1] HATEF DINPARASTI SALEH,[1] KANG LI,[1,3] AND NIGEL COPNER[1,3]

[1] *Wireless & Optoelectronics Research & Innovation Centre (WORIC), Faculty of Computing, Engineering and Science, University of South Wales, Pontypridd, CF37 1DL, United Kingdom*
[2] *School of Physics and Astronomy, Cardiff University, Cardiff, CF24 3AA, United Kingdom*
[3] *Foshan Huikang Optoelectronics Ltd., Foshan 528315, China*
[*] *gongy10@cardiff.ac.uk*

Abstract: We demonstrate tailored thermal radiation in the mid-infrared wavelength range with intriguing capabilities of high emissivity, narrowband spectra, and sharp angular response. The proposed thermal emitter consists of stacking a two-dimensional metallic grating on top of a one-dimensional dielectric Bragg grating (BG). It is interesting to find that the light interaction between the metallic grating and the BG gives rise to impedance matching at wavelengths located in the photonic bandgap of the BG, and allows enhanced polarization-dependent emissivity, selective resonance response, and high radiation directivity. We investigate the plasmonic resonance by exploring various properties and functions including tuning spectral selectivity and tailoring bandwidth at different light polarization and angle of incidence. The developed plasmonic stacked gratings could pave the way towards novel integrated infrared source platforms for various applications such as thermal analysis, imaging, security, biosensing, and medical diagnosis.

1. Introduction

Mid-infrared light is a portion of the electromagnetic spectrum that has found extensive applications ranging from biosensing, military defense, medical diagnosis, imaging, thermophotovoltaics to telecommunications. So far, a variety of advanced mid-infrared light source technologies have been proposed and developed. They can be classified into three types: lasers [1,2], light emitting diodes [3,4], and thermal emitters. Lasers offer high light power, but they are costly, and the operating wavelengths are not always available at the desired wavelengths. Although infrared light emitting diodes are cheaper than lasers, they generally work at wavelengths < 5 μm. Thermal emitters are the most popular approach to generate mid-infrared light attributing to ultrabroad operating wavelengths and much lower cost. In nature, a thermal emitter, such as a black body or an incandescent lamp, is usually incoherent and omnidirectional, which differs fundamentally to a laser that is both temporally and spatially coherent.

Artificial control of thermal radiation that is difficult to attain with natural materials has been a research topic of interest for decades. Plasmonic metamaterials, a class of artificially structured materials, is a promising candidate for manipulating thermal emission properties that are difficult to achieve in natural materials. To date, different types of narrow band metamaterial emitters/absorbers have been reported, such as nano-gratings [5–8], photonic crystals [9–11], thin films [12], and three-layer-metamaterials [13–16]. These proposals have been a strong inspiration for enhancing light-matter interaction and have triggered promising interdisciplinary applications of optical sensors [17–19], hot-electron photodetectors [20], optical modulators [21–25], high-speed switching [26], energy recycling [27–29], image encryption [30,31], to thermal imaging [32]. Among the reported metamaterial thermal emitter technologies, the three-layer metamaterial

#433741 https://doi.org/10.1364/OSAC.433741
Journal © 2021 Received 16 Jun 2021; revised 5 Aug 2021; accepted 6 Aug 2021; published 2 Sep 2021

OSA CONTINUUM

scheme is the most promising arrangement since they support emission features such as a much higher peak and sharper bandwidth than that of a blackbody [33–13]. However, this strategy suffers from a common disadvantage of poor spatial coherence and relatively large spectral bandwidth, which limits the device performance and real-world applications such as ultrahigh resolution optical sensing [35,18].

In this paper, we propose a new kind of thermal emitters based on plasmonic stacked gratings (PSGs) and demonstrate the realization of temporally and spatially coherent thermal radiation. The PSGs are composed of a two-dimensional (2D) metallic nanostructure and a one-dimensional (1D) dielectric Bragg Grating (BG). It is found that the metallic grating acts like a homogeneous slab with large permittivity and small permeability [36], and the interaction between the metallic grating and the BG gives rise to impedance matching at wavelengths located in the photonic band gap of BG, which allows PSGs to perform high emissivity with narrow spectrum and shape angular response in mid-infrared regime. In addition, the operating wavelength, radiation polarization and angle of the PSGs are highly flexible and can be effectively tuned by varying both the BG bandgap and geometry of the metallic gratings. These features open possibilities to obtain a novel compact mid-infrared source scheme that could have great potential for applications such as thermal analysis, imaging, security, biosensing, and medical diagnoses.

2. Concept and Optical Characteristics of the PSGs

The proposed PSGs structure is schematically illustrated in in Fig. 1(a), where a 2D metallic nanostructure with thickness t_m rests on top of a 1D BG arranged in z direction. The BG is composed of two alternately arranged dielectric materials with thicknesses t_a and t_b and refractive indices n_a and n_b, respectively. The total number of grating periods in the BG is denoted as P. The metallic nanostructures are consisted of periodic silver patches with pitches of P_x and P_y along x and y directions. Each silver patch has height of t_m, width of W, and length of L. We investigated absorption properties of the proposed PSGs'. According to the Kirchhoff 's law, the absorptivity of a blackbody equals its emissivity in thermodynamic equilibrium. Therefore, we can tailor the proposed nanostructure absorption to achieve the desired emission properties.

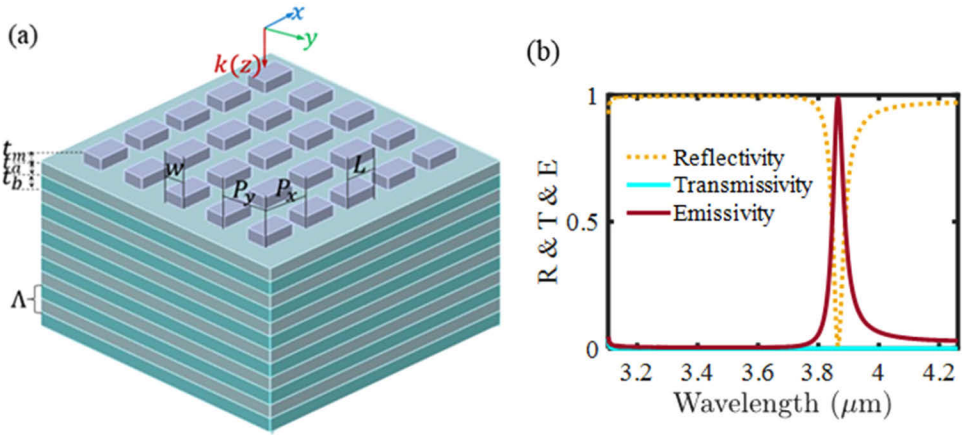

Fig. 1. (a) A schematic diagram of the proposed PSGs composed of 2D metallic nanostructured surface and 1D BG that contains alternative TiO_2 and SiO_2 thin films with a period of Λ. (b) Emissivity, reflectivity, and transmissivity spectrum of the PSGs under normal incidence at TM polarization, where $P_x = P_y = 1.63$ μm, $L = 1.1$ μm, $w = 0.7$ μm, $t_m = 0.05$ μm, $t_a = 0.38$ μm, $t_b = 0.65$ μm, and $P = 20$.

OSA CONTINUUM

We consider TiO_2 and SiO_2 as the dielectric materials in the BG. Three-dimensional finite-difference time-domain (FDTD) method is utilized to design and optimize the proposed PSGs, and the refractive index of all materials are taken from experimental data [37]. The calculated spectrum of the PSGs is plotted in Fig. 1(b). It is noted that a significant resonant dip occurs at a wavelength of 3.86 μm in the reflection spectrum, which results in a narrow-band peak as high as 0.99 in the emissivity spectrum. The physical mechanism of the emergence of the strong and sharp resonance originates from that fact that when a plane wave is impinging on the PSGs along z direction, the 2D silver nanostructure can be equivalently described as a homogeneous slab with frequency-dependent permittivity and permeability [36]. The transmission is negligible at all PSG wavelengths due to the existence of photonic bandgap enabled by the dielectric BG. To get more insight of the behavior of the sharp and strong emissivity, we obtain the emissivity spectra for both TE- and TM-polarized light as well as the reflection and transmission spectra of the BG, as depicted in Fig. 2(a) and 2(b). Clearly, the proposed PSGs support polarization-dependent thermal radiation, which is desirable for various potential applications such as polarization-assisted thermal encryption [29]. We note that the emissivity peaks for both polarizations always appear within the BG bandgap.

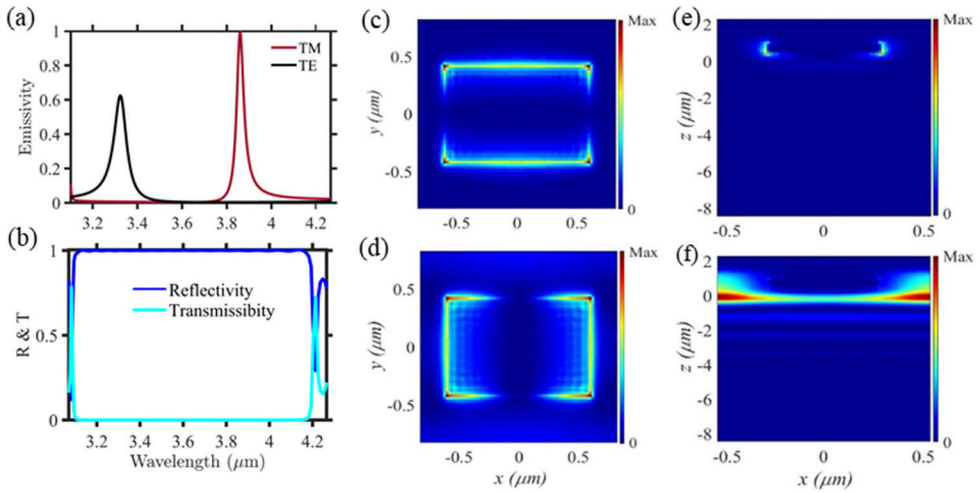

Fig. 2. Polarization-dependent optical characteristics of the PSGs. (a) Emissivity spectra of the PSGs under TE- and TM-polarized incidence of light, respectively. (b) The reflectivity and transmissivity spectra of the BG. Field distribution $|E|^2$ of the PSGs in the central plane (i.e., x-y plane) of the metallic nanostructure at resonant wavelength of 3.32 μm for the TE-polarized light (c) and at resonant wavelength of 3.86 μm for the TM-polarized light (d). Field distribution $|E|^2$ of the PSGs in the x-z plane of the metallic nanostructure at resonant wavelength of 3.32 μm for TE-polarized light (e) and at resonant wavelength of 3.86 μm for TM-polarized light (f). Design parameters are $P_x = P_y = 1.63$ μm, $L = 1.1$ μm, $w = 0.7$ μm, $t_m = 0.05$ μm, $t_a = 0.38$ μm, $t_b = 0.65$ μm, and $P = 20$. For the TE- and TM-polarized incidence of light, the electric fields oscillate along the x and y directions, respectively.

It indicates that the emissivity wavelength can be flexibly tuned by shifting the BG bandgap by means of simply varying the film thickness of the BG. The field distribution of the PSGs at resonant wavelengths are plotted in Fig. 2(c)-(f). It indicates that light is strongly localized and absorbed near the corners of the metallic nanoparticles (Fig. 2(c) and 2(d)), and there is no transmission of light through PSGs (Fig. 2(e) and 2(f)).

OSA CONTINUUM

The relationship between the resonant peaks and the structural parameters of t_m, t_a, t_b, and P_x, P_y is investigated and plotted in Fig. 3. As observed, the resonant wavelength of the PSGs shifts when P_x, P_y rises from 1.63 to 2.03 μm, and the emission peak becomes smaller when the grating period becomes larger than 1.8 μm. The emission wavelength is slightly tunable by varying the BG period, as shown in Fig. 3(a) and (b). We observed the thickness of TiO_2 (t_a) and SiO_2 (t_b) layers in the Bragg gratings plays a crucial role in the emission peak as well as emission wavelength. When thickness t_a varies from 0.33 to 0.43 μm, the emission peak slightly drops to $\sim$ 80%. The BG bandgap position is determined by Bragg condition of $\lambda_{Bragg} = 2(t_a n_a + t_a n_b)$, where λ_{Bragg} is the wavelength of BG bandgap. There, the emission wavelength of the proposed PSGs almost shifts linearly with t_a and t_b, as indicated by Fig. 3(a) and 3(b). The dependence of light emissivity on the thickness of silver film t_m is shown in Fig. 3(d). As t_m increases, the resonant wavelength of the PSGs obviously shift, when the thickness increase from 0.05 to 1 μm. The dependence of transmission and emission at $P = 5$, 10, and 15 are demonstrated in Fig. 3(e) and 3(f), respectively. Hence, the total number of grating periods in the BG (P) would affect the impedance matching condition and cause more transmission through the stacked gratings, only when the number of grating periods of the stack are less than 15. In Fig. 3 (e), when we use a period stack of $P \leq 15$, there is very little transmission, and it does not affect the emission wavelength except the emission intensity. When P is less than 15, there are observed transmission components within the structure, causing less emissivity of the proposed PSGs structure. Therefore, increasing P leads to reduced light transmission through the structure and emission intensity increases.

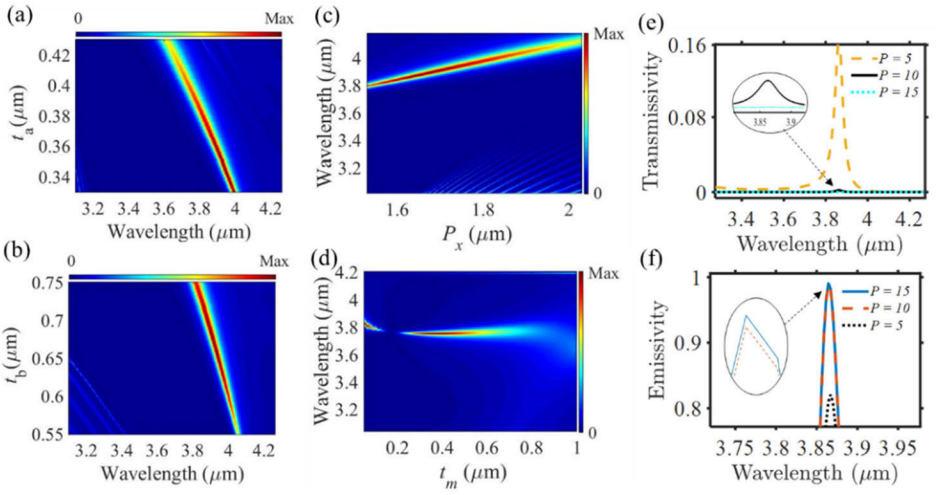

Fig. 3. Evolution of the emissivity spectra to the structure parameters of the PSGs. (a) Dependence of the emissivity spectra on the thickness of TiO_2 when $P_x = P_y = 1.63$ μm, $L = 1.1$ μm, $w = 0.7$ μm, $t_m = 0.05$ μm, $t_b = 0.65$ μm and $P = 20$. (b) Dependence of the emissivity spectra on the thickness of SiO_2 when $P_x = P_y = 1.63$ μm, $L = 1.1$ μm, $w = 0.7$ μm, $t_m = 0.05$ μm, $t_a = 0.38$ μm, and $P = 20$. (c) Dependence of the emissivity spectra on the pitch length when $L = 1.1$ μm, $w = 0.7$ μm, $t_m = 0.05$ μm, $t_a = 0.38$ μm, $t_b = 0.65$ μm, and $P = 20$ (d) Dependence of the emissivity spectra on the thickness of silver film when $P_x = P_y = 1.63$ μm, $L = 1.1$ μm, $w = 0.7$ μm, $t_a = 0.38$ μm, $t_b = 0.65$ μm, and $P = 20$. Transmissibity (e) and emissivity (f) at $P = 5$, 10, 15, when $P_x = P_y = 1.63$ μm, $L = 1.1$ μm, $w = 0.7$ μm, $t_m = 0.05$ μm, $t_a = 0.38$ μm, and $t_b = 0.65$ μm.

OSA CONTINUUM

3. Angular and tunability properties of the PSGs

Attributing to the PSGs' unique property of the emission peak always being located within the band gap of the BG, the FWHM of the PSGs can be flexibly tuned and significantly narrowed by means of decreasing the BG band gap such as by minimizing the refractive index difference of the BG. According to our observations, the emission peak is always located in the BG bandgap. Therefore, when the BG bandgap is narrower, the FWHM of resonant peak would be smaller. Narrowing the BG bandgap relies on minimizing refractive index difference of the BG [36]. In this case, the wavelength range of impedance matching condition becomes narrower. Another intriguing property of the PSGs is spatial directivity. We investigate this property by calculating emission at different angle. Figure 4(a) and (b) illustrate the dependence of the resonant peaks on the radiation angles from 5 deg to 20 deg. The resonant peaks' wavelength varies greatly with angle and the angle bandwidth is quite narrow. As a result, we can observe emission of a single wavelength only at a certain direction. To put it simply, the resonant emission of the proposed PSGs is highly directional. The physical origin for the behavior arises from the fact that the emission wavelengths appear in the BG band gap that is sensitive to the angle of light incidence.

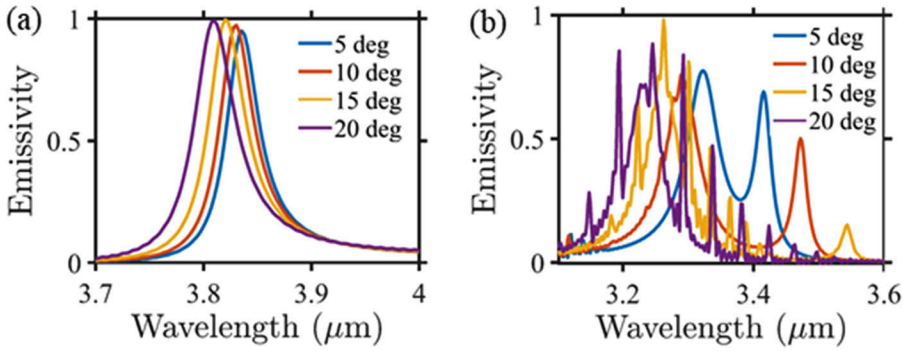

Fig. 4. Angular response of the PSGs. Dependence of the emissivity spectra on the radiation angle for TM-polarized (a) and TE-polarized light (b), respectively. Structure parameters are $P_x = P_y = 1.63\ \mu$m, $L = 1.1\ \mu$m, $w = 0.7\ \mu$m, $t_m = 0.05\ \mu$m, $t_a = 0.38\ \mu$m, $t_b = 0.65\ \mu$m, and $P = 20$.

Finally, we demonstrate that the resonance peaks can be flexible tuned by adjusting the structure parameters. For example, when the nanostructure width w varies from 0.3 μm to 0.7 μm, the

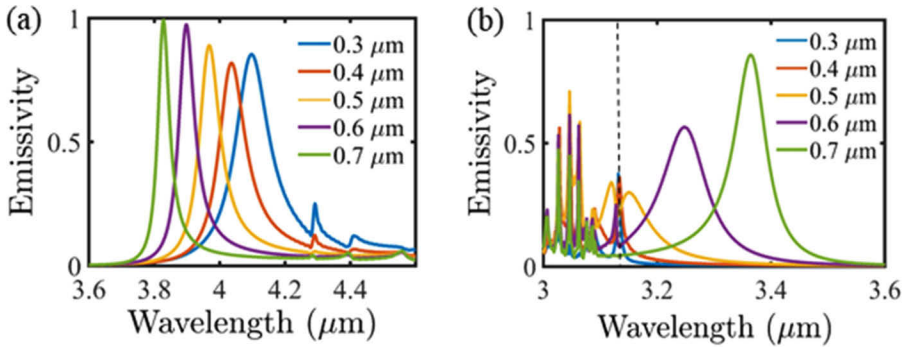

Fig. 5. Tailoring thermal radiation of TM- (a) an TE-polarized light (b) by tuning geometric parameter w from 0.3 μm to 0.7 μm. Other structure parameters are $P_x = P_y = 1.63\ \mu$m, , $L = 1.1\ \mu$m, $w = 0.7\ \mu$m, $t_m = 0.05\ \mu$m, $t_a = 0.38\ \mu$m, $t_b = 0.65\ \mu$m, and $P = 20$.

OSA CONTINUUM

emissivity peak wavelength shifts 3.86 to 4.10 μm for the TM-polarized light and 3.32 μm to 3.15 μm for the TE-polarized light, as depicted in Fig. 5(a) and (b). The dashed line in Fig. 5 (b) indicates the photonic boundary limitation in the spectrum to separate the area that possess zero transmission (right) and non-zero transmission (left) due to polarization changes.

4. Conclusion

In summary, we have proposed a novel PSGs strategy for mid-IR thermal radiation and demonstrate the possibility of enhanced and coherent thermal emission. 3D-FDTD method is utilized to study the spectral and angular emission response of the PSGs. An intriguing characteristic of the thermal emitter scheme is that the emission resonant peaks appear within the bandgap of the BG. Therefore, the FWHM of the emission spectrum can be significantly narrowed by reducing the BG band gap. Replacing the BG with a metallic film could also give rise to a strong resonant emission peak, but the FWHM would be much larger than that of our proposal. In addition, the operating wavelength of the thermal emitter can be flexibly tuned by shifting the bandgap of the BG. These features open possibilities to obtain a cost effective and compact mid-IR source platform. Due to its tunable and narrow spectral and angular response, the PSGs can find potential applications of thermal sensing, security, and infrared diagnoses etc.

Funding. Petroleum Technology Development Fund.

Disclosures. No conflicts of interest

Data availability. Data underlying the results presented in this paper are not publicly available at this time but may be obtained from the authors upon reasonable request.

References

1. S. D. J. N. p. Jackson, "Towards high-power mid-infrared emission from a fibre laser," Nat. Photonics **6**(7), 423–431 (2012).
2. M. R. A. Hassan, F. Yu, W. J. Wadsworth, and J. C. J. O. Knight, "Cavity-based mid-IR fiber gas laser pumped by a diode laser," Optica **3**(3), 218–221 (2016).
3. M. Haigh, G. Nash, S. Smith, L. Buckle, M. Emeny, and T. J. A. p. l. Ashley, "Mid-infrared Al x In 1− x Sb light-emitting diodes," Appl. Phys. Lett. **90**(23), 231116 (2007).
4. L. Meriggi, M. J. Steer, Y. Ding, I. G. Thayne, C. MacGregor, C. N. Ironside, M. J. J. o, and A. P. Sorel, "Enhanced emission from mid-infrared AlInSb light-emitting diodes with p-type contact grid geometry," J. Appl. Phys. **117**(6), 063101 (2015).
5. K. Ikeda, H. Miyazaki, T. Kasaya, K. Yamamoto, Y. Inoue, K. Fujimura, T. Kanakugi, M. Okada, K. Hatade, and S. J. A. P. L. Kitagawa, "Controlled thermal emission of polarized infrared waves from arrayed plasmon nanocavities," Appl. Phys. Lett. **92**(2), 021117 (2008).
6. Y. Qu, Q. Li, H. Gong, K. Du, S. Bai, D. Zhao, H. Ye, and M. J. A. O. M. Qiu, "Spatially and spectrally resolved narrowband optical absorber based on 2D grating nanostructures on metallic films," Adv. Opt. Mater. **4**(3), 480–486 (2016).
7. N. Bonod, G. Tayeb, D. Maystre, S. Enoch, and E. J. O. e. Popov, "Total absorption of light by lamellar metallic gratings," Opt. Express **16**(20), 15431–15438 (2008).
8. H. Sai, Y. Kanamori, and H. J. A. P. L. Yugami, "High-temperature resistive surface grating for spectral control of thermal radiation," Appl. Phys. Lett. **82**(11), 1685–1687 (2003).
9. S.-Y. Lin, J. Moreno, and J. J. A. p. l. Fleming, "Three-dimensional photonic-crystal emitter for thermal photovoltaic power generation," Appl. Phys. Lett. **83**(2), 380–382 (2003).
10. V. Rinnerbauer, A. Lenert, D. M. Bierman, Y. X. Yeng, W. R. Chan, R. D. Geil, J. J. Senkevich, J. D. Joannopoulos, E. N. Wang, and M. J. A. E. M. Soljačić, "Metallic photonic crystal absorber-emitter for efficient spectral control in high-temperature solar thermophotovoltaics," Adv. Energy Mater. **4**(12), 1400334 (2014).
11. J. Fleming, S. Lin, I. El-Kady, R. Biswas, and K. J. N. Ho, "All-metallic three-dimensional photonic crystals with a large infrared bandgap," Nature **417**(6884), 52–55 (2002).
12. N. I. Landy, S. Sajuyigbe, J. J. Mock, D. R. Smith, and W. J. J. P. r. l. Padilla, "Perfect metamaterial absorber," Phys. Rev. Lett. **100**(20), 207402 (2008).
13. X. Liu, T. Tyler, T. Starr, A. F. Starr, N. M. Jokerst, and W. J. J. P. r. l. Padilla, "Taming the blackbody with infrared metamaterials as selective thermal emitters," Phys. Rev. Lett. **107**(4), 045901 (2011).
14. Y. Cui, Y. He, Y. Jin, F. Ding, L. Yang, Y. Ye, S. Zhong, Y. Lin, S. J. L. He, and P. Reviews, "Plasmonic and metamaterial structures as electromagnetic absorbers," Laser Photonics Rev. **8**(4), 495–520 (2014).
15. D. Shrekenhamer, W.-C. Chen, and W. J. J. P. r. l. Padilla, "Liquid crystal tunable metamaterial absorber," Phys. Rev. Lett. **110**(17), 177403 (2013).

OSA CONTINUUM

16. N. Liu, M. Mesch, T. Weiss, M. Hentschel, and H. J. N. l. Giessen, "Infrared perfect absorber and its application as plasmonic sensor," Nano Lett. **10**(7), 2342–2348 (2010).
17. A. Tittl, P. Mai, R. Taubert, D. Dregely, N. Liu, and H. J. N. l. Giessen, "Palladium-based plasmonic perfect absorber in the visible wavelength range and its application to hydrogen sensing," Nano Lett. **11**(10), 4366–4369 (2011).
18. A. Lochbaum, Y. Fedoryshyn, A. Dorodnyy, U. Koch, C. Hafner, and J. J. A. p. Leuthold, "On-chip narrowband thermal emitter for mid-IR optical gas sensing," ACS Photonics **4**(6), 1371–1380 (2017).
19. W. Li and J. J. N. l. Valentine, "Metamaterial perfect absorber based hot electron photodetection," Nano Lett. **14**(6), 3510–3514 (2014).
20. V. W. Brar, M. C. Sherrott, M. S. Jang, S. Kim, L. Kim, M. Choi, L. A. Sweatlock, and H. A. J. N. c. Atwater, "Electronic modulation of infrared radiation in graphene plasmonic resonators," Nat. Commun. **6**(1), 7032–7037 (2015).
21. Y. Miyoshi, Y. Fukazawa, Y. Amasaka, R. Reckmann, T. Yokoi, K. Ishida, K. Kawahara, H. Ago, and H. J. N. c. Maki, "High-speed and on-chip graphene blackbody emitters for optical communications by remote heat transfer," Nat. Commun. **9**(1), 1279–1289 (2018).
22. Y. Yao, R. Shankar, M. A. Kats, Y. Song, J. Kong, M. Loncar, and F. J. N. l. Capasso, "Electrically tunable metasurface perfect absorbers for ultrathin mid-infrared optical modulators," Nano Lett. **14**(11), 6526–6532 (2014).
23. E. Sakat, L. Wojszvzyk, J.-P. Hugonin, M. Besbes, C. Sauvan, and J.-J. J. O. Greffet, "Enhancing thermal radiation with nanoantennas to create infrared sources with high modulation rates," Optica **5**(2), 175–179 (2018).
24. Z. Zhu, P. G. Evans, R. F. Haglund Jr, and J. G. J. N. l. Valentine, "Dynamically reconfigurable metadevice employing nanostructured phase-change materials," Nano Lett. **17**(8), 4881–4885 (2017).
25. T. Inoue, M. De Zoysa, T. Asano, and S. J. A. P. L. Noda, "On-chip integration and high-speed switching of multi-wavelength narrowband thermal emitters," Appl. Phys. Lett. **108**(9), 091101 (2016).
26. W. Li and S. J. O. e. Fan, "Nanophotonic control of thermal radiation for energy applications," Opt. Express **26**(12), 15995–16021 (2018).
27. D. N. Woolf, E. A. Kadlec, D. Bethke, A. D. Grine, J. J. Nogan, J. G. Cederberg, D. B. Burckel, T. S. Luk, E. A. Shaner, and J. M. J. O. Hensley, "High-efficiency thermophotovoltaic energy conversion enabled by a metamaterial selective emitter," Optica **5**(2), 213–218 (2018).
28. M. De Zoysa, T. Asano, K. Mochizuki, A. Oskooi, T. Inoue, and S. J. N. P. Noda, "Conversion of broadband to narrowband thermal emission through energy recycling," Nat. Photonics **6**(8), 535–539 (2012).
29. M. Makhsiyan, P. Bouchon, J. Jaeck, J.-L. Pelouard, and R. J. A. P. L. Haïdar, "Shaping the spatial and spectral emissivity at the diffraction limit," Appl. Phys. Lett. **107**(25), 251103 (2015).
30. G. Bakan, S. Ayas, M. Serhatlioglu, C. Elbuken, and A. J. A. O. M. Dana, "Invisible Thin-Film Patterns with Strong Infrared Emission as an Optical Security Feature," Adv. Opt. Mater. **6**(21), 1800613 (2018).
31. A. Tittl, A. K. U. Michel, M. Schäferling, X. Yin, B. Gholipour, L. Cui, M. Wuttig, T. Taubner, F. Neubrech, and H. J. A. M. Giessen, "A switchable mid-infrared plasmonic perfect absorber with multispectral thermal imaging capability," Adv. Mater. **27**(31), 4597–4603 (2015).
32. W. Li, U. Guler, N. Kinsey, G. V. Naik, A. Boltasseva, J. Guan, V. M. Shalaev, and A. V. J. A. M. Kildishev, "Refractory plasmonics with titanium nitride: broadband metamaterial absorber," Adv. Mater. **26**(47), 7959–7965 (2014).
33. I. Puscasu and W. L. J. A. P. L. Schaich, "Narrow-band, tunable infrared emission from arrays of microstrip patches," Appl. Phys. Lett. **92**(23), 233102 (2008).
34. J. Mason, S. Smith, and D. J. A. P. L. Wasserman, "Strong absorption and selective thermal emission from a midinfrared metamaterial," Appl. Phys. Lett. **98**(24), 241105 (2011).
35. A. Lochbaum, A. Dorodnyy, U. Koch, S. M. Koepfli, S. Volk, Y. Fedoryshyn, V. Wood, and J. Leuthold, "Compact Mid-Infrared Gas Sensing Enabled by an All-Metamaterial Design," Nano Lett. **20**(6), 4169–4176 (2020).
36. Y. Gong, X. Liu, K. Li, J. Huang, J. J. Martinez, D. Rees-Whippey, S. Carver, L. Wang, W. Zhang, T. Duan, and N. Copner, "Coherent emission of light using stacked gratings," Phys. Rev. B **87**(20), 205121 (2013).
37. E. D. Palik, *Handbook of optical constants of solids* (Academic, San Diego, Calif., 1998), Vol. 3.